

# The influence of non-anchored polymers on the curvature of vesicles¶

MARKUS BREIDENICH†, ROLAND R. NETZ‡ and REINHARD LIPOWSKY\*§

†European Patent Office, 80298 München, Germany

‡Physik Department, Technische Universität München, 85748 Garching, Germany

§Max-Planck-Institute of Colloids and Interfaces, 14424 Potsdam, Germany

(Received 29 April 2005; in final form 21 July 2005)

The influence of non-anchored polymers on the membrane curvature of vesicles is studied theoretically. The interaction between polymer and membrane consists of a hard-wall contribution, which prevents the polymer from penetrating the membrane, and an additional attractive potential which can lead to polymer adsorption onto the membrane surface. The vesicle membrane divides space into an interior and an exterior compartment. These two compartments are taken to be osmotically balanced but may contain different polymer species. The polymer-induced curvature of the vesicle membrane is calculated as a function of the adsorption strength which is described by the inverse extrapolation length. For strong adsorption, the membrane bends away from the adsorbed polymers whereas it bends towards the polymers for complete desorption. The polymer-induced curvature changes its sign at a characteristic adsorption strength below the adsorption transition which corresponds to a positive value of the inverse extrapolation length.

## 1. Introduction

Composite systems, which contain polymers, nanoparticles, or colloids in contact with fluid membranes, form simple models for biological membranes and are promising candidates for biotechnological applications [1]. Explicit experimental examples include polymers which are attached to membranes via lipid/hydrophobic anchors [2, 3] as well as water-soluble polymers which are confined in lamellar membrane stacks [4]. A separate line of experimental research has been performed on the growth of nanoparticles in closed membrane shells [5, 6].

From the theoretical point of view, one should distinguish several distinct systems. The presumably simplest situation is provided by polymers which are *anchored* with one end to the membranes. Each anchored polymer suffers a loss of *configurational entropy* by the presence of the membrane [7]. If all other polymer segments experience effectively repulsive interactions with the membrane, the polymer forms a mushroom which entropically bends the membrane away from it [7–12]. In addition, the polymer mushrooms increase the bending rigidity of the

membranes [8, 12]. The latter effect has been confirmed experimentally [13]. Another mechanism for the generation of membrane curvature is provided by ensembles of anchored molecules which are rigid but undergo collisions because of their lateral diffusion within the membranes [10, 14].

If the polymer–membrane interaction contains a sufficiently strong attractive part, the anchored polymers form adsorbed pancakes on the membranes which can bend towards or away from the polymers [9, 15–17]. This non-universality was first found for spherical and conical membrane segments with a curvature-dependent extrapolation length [9, 15]. A self-consistent calculation of the membrane shape in the presence of the adsorbed polymers showed that the sign of the polymer-induced curvature depends on the relative size of the anchor segment and the range of the attractive polymer–membrane interaction [16]. In all cases, the membrane curvature *decreases monotonically* as one increases the strength of this attractive interaction (using the convention that the membrane curvature is positive and negative if the membrane bends away from and towards the anchored polymer, respectively).

In the present article, we consider aqueous solutions of vesicles and dispersed polymers *without* any anchor segments. The vesicle membranes are impermeable for

\*Corresponding author. Email: lipowsky@mpikg.mpg.de

¶Dedicated to Ben Widom.

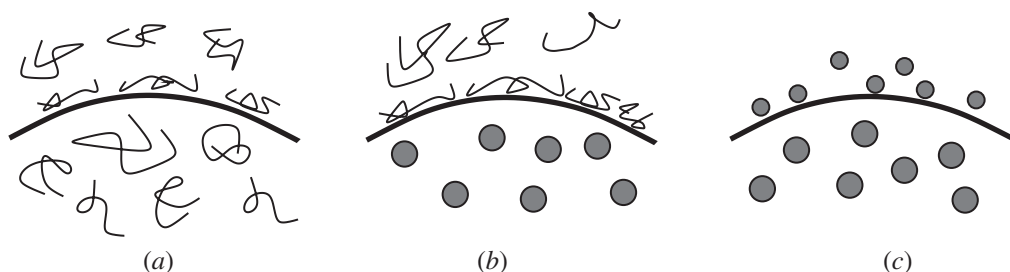


Figure 1. Three different systems with a membrane separating an exterior (up) and an interior (down) vesicle compartment: (a) the exterior compartment contains adsorbing polymers whereas the interior compartment contains desorbing ones. In this case, the membrane bends away from the adsorbed polymers and towards the desorbed polymers. (b) The polymers are adsorbed on the membrane, whereas the colloids are desorbed. The membrane bends again away from the adsorbed polymers. (c) Two different types of nanoparticles: the membrane bends away from the adsorbing and/or smaller particles.

the polymers which implies that the polymers in the interior vesicle compartments cannot explore the exterior compartment and vice versa. Therefore, the presence of the vesicles leads to an additional loss of *translational entropy* for the dissolved polymers. This translational entropy loss does not depend on the internal structure of the dissolved particles and, thus, is also present for rigid nanoparticles or dispersion colloids.

The *non-anchored* particles may be repelled from or attracted towards the membrane surfaces. If these particles are repelled from the membranes, depletion layers are formed in front of these membranes which increase the excess free energies of the membrane–water interfaces [18]. In such a situation, the membranes bend towards the particle solution in order to decrease the size of the depletion zone [19, 20]. On the other hand, if relatively small particles are adsorbed onto the membrane, the Gibbs adsorption equation implies that the membrane tends to bend away from the particle solution in order to increase its area [20]†.

In general, the two spatial compartments, which are separated by the membrane, may contain identical or different polymer solutions. For the symmetric case with identical polymer solutions on both sides of the membrane, the polymers do not induce any ‘spontaneous’ membrane curvature, and their main effect is to modify the membrane’s bending rigidity. This effect has been studied by molecular field theories [21–24], perturbation expansions [25] and computer simulations [26]. On the other hand, for the asymmetric case, the two compartments contain distinct polymer solutions and a ‘spontaneous’ curvature will be induced in the membrane. The latter situation was studied for ideal polymers in [27] but this study concluded that membranes bend away from non-anchored polymers if these polymers are *not* adsorbed onto the membranes.

However, subsequent theoretical studies both for ideal [19, 28] and for non-ideal polymers [19] led to the opposite sign for the polymer-induced curvature.

In this article, we will reconsider this asymmetric situation, i.e. we will consider mixtures of vesicles and non-anchored polymers for which the interior and exterior vesicle compartments contain different aqueous solutions. The specific situation which we have in mind corresponds to vesicles which have been prepared in a certain polymer solution and are subsequently transferred to another solution. We will study the dependence of the polymer-induced membrane curvature on the polymer–membrane interactions which we vary from purely repulsive to strongly attractive. We find that the *membrane bends towards the non-adsorbing polymers but bends away from the adsorbing ones*. This implies that there is an intermediate adsorption strength at which the polymer-induced curvature changes its sign.

Within our theoretical models, the strength of the attractive polymer–membrane interactions is described by the so-called extrapolation length [29, 30]. Since these interactions may differ on the two sides of the membranes, we consider the general situation of two different extrapolation lengths for the interior and exterior vesicle compartments. The polymers are taken to behave as ideal chains corresponding to the experimentally accessible case of polymers in  $\theta$ -solvents for which the excluded volume interactions between the polymer segments are balanced by their attractive interactions.

In addition to polymer solutions, we also treat solutions of spherical nanoparticles or colloids as previously considered in [20]. Therefore, our theoretical results apply to a variety of dispersions as shown in figure 1: (i) both the interior and the exterior vesicle compartments contain dissolved polymers as in

†The size of these particles should be small compared to the membrane thickness; otherwise, the membranes will tend to wrap around the particles.

figure 1 (a); (ii) these two types of compartments contain rigid nanoparticles and polymers, respectively, as in figure 1 (b); and (iii) both types of compartments contain spherical nanoparticles or colloids, as in figure 1(c).

In cases (i) and (ii), the polymers lose both translational and configurational entropy by the presence of the non-permeable membranes. In case (iii), the spherical nanoparticles lose translational entropy only and we recover the results of [20].

Our article is organized as follows. In section 2, we define the partition function of a single polymer chain in contact with a vesicle membrane. We first discuss general polymer–membrane interactions and then introduce the extrapolation length for the attractive part of these interactions. In sections 3 and 4, we calculate the partition function for a single polymer chain which can explore the whole exterior or interior vesicle compartment. We will describe two different calculational methods which give identical results. In section 5, we generalize our results to polymer solutions characterized by different chemical potentials. The corresponding partition functions for colloidal dispersions are discussed in section 6. Finally, section 7 describes our main results for the membrane curvature induced by non-anchored polymers and colloids.

## 2. Single polymer chain close to spherical vesicle

We first consider a single polymer chain close to a spherical vesicle. The polymer is characterized by its end-to-end distance which is denoted by  $R_{p,ex}$  and  $R_{p,in}$  if it is located within the exterior or interior vesicle compartment, respectively. Since the chain is taken to be ideal, the end-to-end distance satisfies the relation

$$R_p = a_p N^{1/2}, \quad (1)$$

where  $a_p$  denotes the Kuhn length and  $N$  is the number of monomers or statistically independent polymer segments.

In this section, we determine the partition function of a single chain with one of its ends anchored in the exterior compartment. The anchor point is *not* located on the vesicle membrane but has an arbitrary distance from this membrane. In the next section, we will then sum over all possible locations of this anchor point.

In the following, we start from the situation of a polymer chain for which both ends have a fixed location and then integrate over all configurations of one end. We show how the corresponding partition function for a curved membrane surface can be transformed into the one for a planar membrane surface. Finally, we describe

the attractive polymer–membrane interaction in terms of the extrapolation length.

### 2.1. Path integral representation of partition function

Let us first consider a single, ideal polymer chain in the presence of a force potential  $V$  which corresponds to the potential energy per monomer or bead. The spatial position of the beads is described by the Cartesian coordinates  $\mathbf{r} = (r_1, r_2, r_3)$ . If the two end points of the polymer are fixed at  $\mathbf{r} = \mathbf{r}_0$  and  $\mathbf{r} = \mathbf{r}_N$ , the reduced partition function  $\bar{Z}$  of the polymer satisfies the Schrödinger-type equation as given by

$$\left[ \frac{\partial}{\partial N} - \frac{a_p^2}{6} \Delta_{\mathbf{y}} + \frac{V(\mathbf{y})}{T} \right] \bar{Z}(\mathbf{r}_0, 0 | \mathbf{y}, N) = 0 \quad \text{with } \mathbf{y} \equiv \mathbf{r}_N, \quad (2)$$

where  $N$  is the total bead number,  $a_p$  is the Kuhn length and  $T$  is the temperature in energy units. This differential equation is supplemented by the ‘initial’ condition

$$\bar{Z}(\mathbf{r}_0, 0 | \mathbf{r}_N, N \equiv 0) = \delta(\mathbf{r}_0 - \mathbf{r}_N). \quad (3)$$

The solution of the Schrödinger-type equation (2) together with the ‘initial’ condition (3) is given by the path integral

$$\bar{Z}(\mathbf{r}_0, 0 | \mathbf{r}_N, N) = \int \mathcal{D}'\{\mathbf{r}\} \exp \left( -\frac{3}{2a_p^2} \int_0^N dn \left[ \frac{d}{dn} \mathbf{r}(n) \right]^2 - \int_0^N dn \frac{V(\mathbf{r}(n))}{T} \right) \quad (4)$$

with the abbreviation

$$\int \mathcal{D}'\{\mathbf{r}\} \equiv \int \mathcal{D}\{\mathbf{r}\} \delta[\mathbf{r}(0) - \mathbf{r}_0] \delta[\mathbf{r}(N) - \mathbf{r}_N], \quad (5)$$

where the internal coordinate  $n$  of the chain varies between 0 to  $N$ . We now change variables from  $n$  to the contour length  $s \equiv n/N$  with  $0 \leq s \leq 1$ , and sum the partition function over all possible positions  $\mathbf{r}_N$  of the second polymer end. This leads to the new partition function

$$Z(\mathbf{r}_0) = \int \mathcal{D}\{\mathbf{r}\} \delta[\mathbf{r}(0) - \mathbf{r}_0] \exp \left( -\frac{3}{2R_p^2} \int_0^1 ds \left[ \frac{d}{ds} \mathbf{r}(s) \right]^2 - \int_0^1 ds \frac{V(\mathbf{r}(s))}{T} \right) \quad (6)$$

for an ideal polymer chain with one of its ends anchored at  $\mathbf{r} = \mathbf{r}_0$ , where  $R_p \equiv a_p N^{1/2}$  denotes its end-to-end distance as in (1).

## 2.2. Polymer chain with one anchored end point

The path integral representation of the partition function as discussed in the previous subsection is rather general and applies to any geometry. We will now focus on the situation in which the force potential arises from the membrane of a spherical vesicle with radius  $R$ , as shown in figure 2. The centre of the spherical vesicle surface is placed at the origin of the Cartesian coordinate system with  $\mathbf{r} = (0, 0, 0)$ . In addition, this coordinate system is rotated in such a way that the anchored end point of the polymer is located on the  $r_3$  axis with

$$\mathbf{r}_0 = (0, 0, r_3) \equiv (0, 0, R_0), \quad (7)$$

see figure 2. We will also use the notation  $\underline{r} = (r_1, r_2)$  for the two Cartesian coordinates perpendicular to  $r_3$ .

The vesicle membrane partitions space into two separate compartments, the interior and the exterior compartments which will be indicated by the subscripts ‘in’ and ‘ex’. In the next subsections, we will first discuss the situation in which the polymer is located in the exterior compartment as shown in figure 2. The corresponding partition function is denoted by  $Z_{\text{ex}}(R_0)$ .

In order to calculate  $Z_{\text{ex}}(R_0)$ , we will apply a small curvature expansion as developed previously in [10, 16] which applies to the limit of large vesicle radius  $R \gg R_p$ . In this latter limit, a polymer chain which is

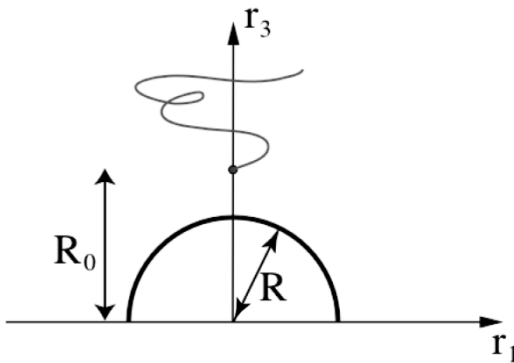


Figure 2. Single polymer in the exterior compartment outside a spherical vesicle of radius  $R$ . One end of the polymer is anchored at distance  $R_0$  from the origin of the coordinate system. The latter system is chosen in such a way that the anchor point has the lateral coordinate  $\underline{r}(0) = (r_1(0), r_2(0)) = (0, 0)$  and, thus,  $r_3 = R_0$ . The difference  $R_0 - R$ , i.e. the distance of the anchored end from the membrane surface will be denoted by  $\rho_0$ .

anchored above the ‘north pole’ of the spherical vesicle, see figure 2, will not explore the lower half space with  $r_3 < 0$ . It is then convenient to consider the auxiliary surface as defined via

$$l(\underline{r}) \equiv \begin{cases} R(1 - \underline{r}^2/R^2)^{1/2} & \text{for } |\underline{r}| \leq R, \\ 0 & \text{for } |\underline{r}| > R. \end{cases} \quad (8)$$

The surface as defined by (8) is taken to be impenetrable for the polymer chain. In addition, the spherical surface corresponding to the vesicle membrane exerts a short-ranged attractive potential onto the polymer beads. Thus, a bead located at  $\mathbf{r}$  experiences the attractive potential  $V_a(|\mathbf{r}| - R)$  which depends on the distance,  $|\mathbf{r}| - R$ , of the bead from the spherical surface. In the limit of small curvature  $1/R$ , this distance behaves as

$$\begin{aligned} |\mathbf{r}| - R &\approx r_3 - l(\underline{r}) + \frac{1}{2}(r_1^2 + r_2^2) \left( \frac{1}{r_3} - \frac{1}{R} \right) \\ &\approx r_3 - l(\underline{r}) - \frac{1}{2}(r_1^2 + r_2^2) \frac{\Delta r_3}{R^2} \end{aligned} \quad (9)$$

with  $\Delta r_3 \equiv r_3 - R$  which is of order  $\mathcal{O}(R^0)$ . Thus, the short-ranged attractive potential  $V_a$  behaves as

$$V_a(|\mathbf{r}| - R) = V_a(r_3 - l(\underline{r})) + \mathcal{O}(1/R^2) \quad (10)$$

for small curvatures  $1/R$ . Since we will limit our calculation to first order in  $1/R$ , we can simply replace  $V_a(|\mathbf{r}| - R)$  by  $V_a(r_3 - l(\underline{r}))$  as will be done in the following.

In this way, we arrive at the partition function

$$\begin{aligned} Z_{\text{ex}}(R_0) &= \int \mathcal{D}'\{\mathbf{r}\} \exp \left( -\frac{3}{2R_{\text{p,ex}}^2} \int_0^1 ds \left[ \frac{d}{ds} \mathbf{r} \right]^2 \right. \\ &\quad \left. - \int_0^1 ds \frac{V_a(r_3 - l(\underline{r}))}{T} \right) \end{aligned} \quad (11)$$

with the abbreviation

$$\int \mathcal{D}'\{\mathbf{r}\} \equiv \int_{-\infty}^{\infty} \mathcal{D}[\underline{r}] \delta[\underline{r}(0)] \int_{l(\underline{r})}^{\infty} \mathcal{D}\{r_3\} \delta[r_3(0) - R_0], \quad (12)$$

where  $R_{\text{p,ex}}$  is the end-to-end distance in the exterior compartment which may, in general, differ from the corresponding distance in the interior compartment. Note that the hard-wall interaction between the polymer

beads and the membrane surface has been incorporated by the lower bound  $l(r)$  for the integration over the displacement field  $r_3$ .

We will now change variables from  $r_3$  to  $r'_3 \equiv r_3 - l(r)$  and use the small curvature expansion  $l(r) = R - r^2/2R + \mathcal{O}(R^{-3})$  which follows from the definition (8) of the height variable  $l$ . As a result, we obtain the expression

$$Z_{\text{ex}}(R_0) = \int \bar{\mathcal{D}}\{L\} \int \bar{\mathcal{D}}\{r_3\} \exp\left(-\frac{3}{2R_{\text{p,ex}}^2} \int_0^1 ds \left[\frac{d}{ds}r(s)\right]^2\right) \times \exp\left(-\frac{3}{2R_{\text{p,ex}}^2} \int_0^1 ds \left[r_3(s) - \frac{r(s)^2}{2R}\right]^2\right) - \int_0^1 ds \frac{V_a(r_3)}{T} \quad (13)$$

with

$$\int \bar{\mathcal{D}}\{L\} \equiv \int_{-\infty}^{\infty} \mathcal{D}\{L\} \delta[L(0)] \quad \text{and} \quad \int \bar{\mathcal{D}}\{r_3\} \equiv \int_0^{\infty} \mathcal{D}\{r_3\} \delta[r_3(0) - R_0], \quad (14)$$

where the dummy variable  $r'_3$  was again denoted by  $r_3$ . Note that the partition function (13) has two appealing properties: (i) the variable  $r_3 = r_3(s)$  is now restricted to the half space with  $r_3 > 0$ ; and (ii) the vesicle radius  $R$  enters only via the ‘gradient’ term  $[(d/ds)(r_3(s) - r(s)^2/2R)]^2$ . Note also that the vesicle radius  $R$  and the anchor distance  $R_0$ , which both enter the above expression for the partition function  $Z_{\text{ex}}(R_0)$ , satisfy  $R < R_0$ .

### 2.3. Contact potential and extrapolation length

In general, the attractive potential  $V_a$  between the membrane surface and the polymer beads will depend on many parameters. In order to reduce the number of these parameters, we will now consider the limit of a contact potential which is characterized by a single parameter, namely the extrapolation length  $\ell_e$  [29, 30]. In this case, the Schrödinger-type equation (2) does not contain any potential term but is supplemented by an additional boundary condition at the membrane surface which depends on  $\ell_e$ .

In general, the extrapolation length scale may differ on the two sides of the membranes and we will, thus, distinguish  $\ell_{e,\text{in}}$  from  $\ell_{e,\text{ex}}$ . For the exterior compartment, the boundary condition for the partition function

is then given by

$$\hat{\mathbf{n}} \cdot \nabla_{\mathbf{r}} \bar{Z}_{\text{ex}}(\mathbf{r}_0, 0 | \mathbf{r}_N, N) = \bar{Z}_{\text{ex}}(\mathbf{r}_0, 0 | \mathbf{r}_N, N) / \ell_{e,\text{ex}} \quad \text{for } \mathbf{r}_N \text{ located on the surface,} \quad (15)$$

where  $\hat{\mathbf{n}}$  is the normal vector on the membrane surface pointing into the outer polymer solution. The corresponding boundary condition for the interior compartment is obtained if we replace  $\ell_{e,\text{ex}}$  by  $\ell_{e,\text{in}}$  and change the direction of the normal vector  $\hat{\mathbf{n}}$ .

In the case of a purely steric repulsion, i.e. in the desorption regime, the polymers are repelled from the membrane surface, leading to a depletion zone in which the monomer density decreases. In the limit of strong adsorption, the polymers prefer to be close to the membrane surface. Consequently, the monomer density in the vicinity of the membrane increases and the polymers form an adsorption layer on the membrane. In contrast to the situation of anchored polymers, where the bending of the membrane is governed by the changes in the configurational entropy of the polymer [7, 8, 10, 11, 16], in the case of non-anchored polymers studied here, the curvature is governed by both the configurational and the translational entropy of the polymers. The desorption limit of purely steric interaction corresponds to large positive  $1/\ell_{e,\text{ex}}$ , whereas the adsorption limit corresponds to large negative  $1/\ell_{e,\text{ex}}$ . Both regimes are separated by the adsorption–desorption transition at  $1/\ell_{e,\text{ex}} = 0$ . Note, that this transition is a genuine phase transition only in the limit of an infinitely long chain. For finite chain lengths and finite concentration, the adsorption and desorption regimes are distinguished by increased and decreased monomer densities in the vicinity of the membrane.

### 3. Curvature expansion of partition function

In order to calculate the effect of a polymer on the membrane curvature, we will now study the dependence of the polymer partition function on the vesicle radius  $R$ . As previously mentioned, the partition function (13) depends on  $R$  only via the ‘gradient’ term  $[(d/ds)(r_3(s) - r(s)^2/2R)]^2$ . It is then straightforward to expand this expression for the partition function in powers of  $1/R$  which corresponds to a small curvature expansion.

If the polymer is anchored in the exterior compartment, the radius  $R_0$  of the anchor point must satisfy  $R_0 > R$ , see figure 2. It is now convenient to define the shifted radius

$$\rho_0 \equiv R_0 - R \quad (16)$$

of the anchor point and to keep  $\rho_0$  fixed as both  $R$  and  $R_0$  go to infinity.

As a result, one obtains

$$Z_{\text{ex}}(R + \rho_0) = \sum_{n=0}^{\infty} \frac{1}{n!} Z_{\text{ex}}^{(n)}(\rho_0) R^{-n} \quad \text{with}$$

$$Z_{\text{ex}}^{(n)} \equiv \left. \frac{d^n Z_{\text{ex}}}{d(1/R)^n} \right|_{1/R=0}. \quad (17)$$

The first,  $R$ -independent term of this expansion is given by

$$Z_{\text{ex}}^{(0)}(\rho_0) = \int_{-\infty}^{\infty} d^2x_e Z_{\text{fr}}(\underline{Q}|\underline{x}_e, 1)$$

$$\int_0^{\infty} dz_e Z_{\text{hs}}^{\ell_{e,\text{ex}}}(\rho_0|z_e, 1), \quad (18)$$

where the coordinate  $(x_e, z_e)$  represents the location of the end-point of the polymer. In the lateral directions, the polymer moves freely and is thus described by the free space partition function as given by

$$Z_{\text{fr}}(\underline{Q}|\underline{x}, s) = \frac{3}{2\pi s} \frac{1}{R_{\text{p,ex}}^2} \exp\left(-\frac{3}{2s} \frac{x^2}{R_{\text{p,ex}}^2}\right). \quad (19)$$

In the perpendicular direction, the movement of the monomers is restricted to the half space (hs). The corresponding partition function reads [31]

$$Z_{\text{hs}}^{\ell_{e,\text{ex}}}(\rho_0|z, s)$$

$$= \left(\frac{3}{2\pi s}\right)^{1/2} \frac{1}{R_{\text{p,ex}}} \left[ \exp\left(-\frac{3}{2s} \frac{(z - \rho_0)^2}{R_{\text{p,ex}}^2}\right) \right.$$

$$\left. + \exp\left(-\frac{3}{2s} \frac{(z + \rho_0)^2}{R_{\text{p,ex}}^2}\right) \right]$$

$$- \frac{1}{\ell_{e,\text{ex}}} \exp\left(\frac{R_{\text{p,ex}}^2}{6\ell_{e,\text{ex}}^2} s + \frac{z + \rho_0}{\ell_{e,\text{ex}}}\right)$$

$$\times \operatorname{erfc}\left(\frac{R_{\text{p,ex}}}{\ell_{e,\text{ex}}} \left(\frac{s}{6}\right)^{1/2} + \left(\frac{3}{2s}\right)^{1/2} \frac{z + \rho_0}{R_{\text{p,ex}}}\right), \quad (20)$$

in which, according to (15), the contact potential has been replaced by the characteristic extrapolation length  $\ell_{e,\text{ex}}$  for the half-space. Here and below, the symbol  $\operatorname{erfc}$  denotes the complementary error function

$$\operatorname{erfc}(x) \equiv \frac{2}{\pi^{1/2}} \int_x^{\infty} dt \exp(-t^2)$$

$$\approx \exp(-x^2)/\pi^{1/2} x \quad \text{for large } x. \quad (21)$$

In the perpendicular direction of equation (18), the integration with respect to the polymer endpoint  $Z_{\text{hs}}^{\ell_{e,\text{ex}}}(\rho_0) := \int_0^{\infty} dz_e Z_{\text{hs}}^{\ell_{e,\text{ex}}}(\rho_0|z_e, 1)$  yields the probability of finding the starting point of the polymer at a distance  $\rho_0$  from the planar wall. Far away, this probability is 1 due to the normalization of the partition function. Close to the surface, the probability will decrease in the case of desorption and increase in the case of adsorption. Thus, for large values of  $z_0$  the integrated partition function  $Z_{\text{hs}}^{\ell_{e,\text{ex}}}(\rho_0)$  leads to the bulk behaviour, whereas for small values of  $\rho_0$  one finds the desorption/adsorption behaviour.

Insertion of the two partition functions into (18) then leads to

$$Z_{\text{ex}}^{(0)}(\rho_0) = 1 + \Delta Z_{\text{ex}}^{(0)}(\rho_0) \quad (22)$$

with

$$\Delta Z_{\text{ex}}^{(0)}(\rho_0) \equiv -\operatorname{erfc}\left(\left(\frac{3}{2}\right)^{1/2} \frac{\rho_0}{R_{\text{p,ex}}}\right)$$

$$+ \operatorname{erfc}\left(\frac{R_{\text{p,ex}}}{6^{1/2}\ell_{e,\text{ex}}} + \left(\frac{3}{2}\right)^{1/2} \frac{\rho_0}{R_{\text{p,ex}}}\right)$$

$$\times \exp\left(\frac{R_{\text{p,ex}}^2}{6\ell_{e,\text{ex}}^2} + \frac{\rho_0}{\ell_{e,\text{ex}}}\right). \quad (23)$$

The asymptotic behaviour of the complementary error function as given by (21) implies that

$$Z_{\text{ex}}^{(0)}(\rho_0) \approx 1 \quad \text{for large } \rho_0. \quad (24)$$

In the next section, we will consider non-anchored polymers and, thus, integrate over the anchor radius  $R_0$  or  $\rho_0 = R_0 - R$  respectively. Because of (24), the leading term obtained from this integration is proportional to the exterior volume.

In the next order, the expansion of (13) in powers of  $1/R$  leads to the first-order term

$$Z_{\text{ex}}^{(1)}(\rho_0) = \frac{3}{R_{\text{p,ex}}^2} \int_0^1 ds \frac{d}{ds} \left[ \int \bar{\mathcal{D}}\{r\} \frac{r(s)^2}{2} \right.$$

$$\left. \times \exp\left(-\frac{3}{2R_{\text{p,ex}}^2} \int_0^1 ds \left[\frac{d}{ds} r(s)\right]^2\right) \right]$$

$$\times \frac{d}{ds} \left[ \int \bar{\mathcal{D}}\{r_3\} r_3(s) \exp\left(-\frac{3}{2R_{\text{p,ex}}^2} \int_0^1 ds \left[\frac{d}{ds} r_3(s)\right]^2 \right) \right.$$

$$\left. - \int_0^1 ds V[r_3(s)] \right], \quad (25)$$

where the integration symbols have been defined in (14). Integrating out the polymer degrees of freedom leads to the first-order term

$$\begin{aligned} Z_{\text{ex}}^{(1)}(\rho_0) &= \left[ \int_0^\infty dz \int_0^\infty dz_e Z_{\text{hs}}^{\ell_{\text{e,ex}}}(\rho_0|z, s) z Z_{\text{hs}}^{\ell_{\text{e,ex}}}(z|z_e, 1-s) \right]_{s=0}^1 \\ &= -(\rho_0 + \ell_{\text{e,ex}}) \Delta Z_{\text{ex}}^{(0)}(\rho_0) \end{aligned} \quad (26)$$

with  $\Delta Z_{\text{ex}}^{(0)}$  as defined in (23).

#### 4. Non-anchored polymer chain close to spherical vesicle

So far, we have considered a single polymer that is anchored at one of its ends which has the fixed distance  $R_0$  from the origin or  $\rho_0 = R_0 - R$  from the membrane surface, see figure 2. In the present section, we will now allow this end to move in a certain exterior volume  $\mathcal{V}_{\text{ex}}$  around the vesicle and, thus, consider non-anchored polymer chains.

For anchored polymers, the bending of the membrane is governed by the configurational entropy of the polymer [7, 8, 10, 11, 16]. For non-anchored polymers, the situation is more complex since the curvature is now governed by both the configurational and the translational entropy of the polymers. In order to avoid over-counting of polymer configurations, we assume, that the polymer starting and end-point are chemically different and thus distinguishable. However, both ends are taken to experience the same monomer–membrane interaction.

##### 4.1. Geometry

If we move the anchored polymer far away from the membrane, the anchor distance  $R_0$  becomes large and the polymer partition function becomes equal to one as in (24). Therefore, in order to obtain a finite integral, we now restrict the integral over all possible positions of the anchored end by introducing an auxiliary spherical surface with radius  $R + L$  as shown in figure 3.

Inspection of figure 3 shows that the exterior compartment is now bounded by the spherical vesicle surface with radius  $R$  and by the spherical auxiliary surface with radius  $R + L$ . Therefore, the distance  $R_0$  of the anchored end from the origin of the coordinate system is now restricted to  $R < R_0 < R + L$ . The spherical membrane surface is impenetrable for all segments of the polymers. In contrast, the spherical auxiliary surface with radius  $R + L$  is only impenetrable for the ‘starting’ end-point of the polymers but is penetrable for the remaining segments of the polymer chains. We will calculate the partition function for finite

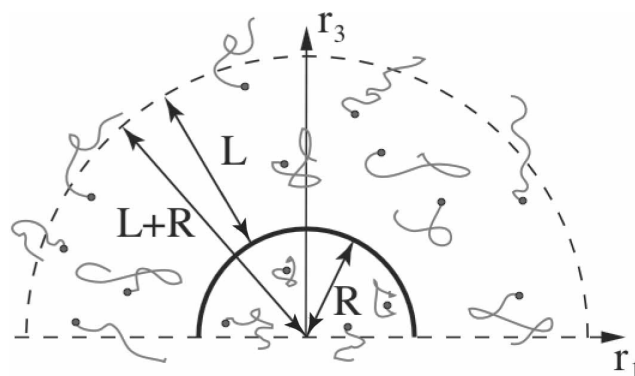


Figure 3. Spherical vesicle of radius  $R$  in contact with two polymer solutions. In general, the interior and exterior compartments will contain different polymers. In order to define the system in such a way that it has a well-defined thermodynamic limit, the exterior volume is bounded by a spherical surface (dashed) of radius  $L + R$ . The latter surface represents a hard, impenetrable wall for one end-point of the polymers (filled circle) but is penetrable for the remaining segments of the polymer chains. The vesicle surface (thick line) is impenetrable for all polymer segments. Only one half space of the system is shown. For a polymer chain anchored at the  $r_3$  axis with  $r_3 = R_0 > R$  as in figure 2, the other half space below the dashed horizontal line plays no role. However, when integrating over  $R_0$ , we include both half spaces.

$L$  and then define an appropriate excess quantity that is finite in the limit of large  $L$ .

##### 4.2. Small curvature expansion

The partition function of a freely moving polymer in the exterior volume is given by

$$\mathcal{Z}_{\text{ex}}^{(L)} = 4\pi \int_0^L d\rho_0 (R + \rho_0)^2 Z_{\text{ex}}(R + \rho_0). \quad (27)$$

As before, the partition function  $Z_{\text{ex}}(R + \rho_0)$  corresponds to a single polymer with one end-point fixed at  $R + \rho_0 = R_0 > R$  in the exterior compartment.

As explained before, see figure 3, only the spherical membrane surface of radius  $R$  is impenetrable for the polymer chains and therefore leads to configurational changes of the polymers in its vicinity. The outer sphere provides a boundary only for the translational motion of the polymers in the bulk and, thus, only for one of its end points, see figure 3. Thus, in order to perform the limit of large  $L$ , one must first subtract the volume part corresponding to the translational movements of the polymer in the bulk system. In this limit, one obtains the partition function difference

$$\Delta \mathcal{Z}_{\text{ex}} = 4\pi \int_0^\infty d\rho_0 (R + \rho_0)^2 [Z_{\text{ex}}(R + \rho_0) - 1], \quad (28)$$

which is independent of  $L$ .

Inserting the expansion of the polymer partition function  $Z_{\text{ex}}(R + \rho_0)$  as given by (17), (22) and (26) into expression (28), we obtain

$$\Delta Z_{\text{ex}} \approx 4\pi \int_0^\infty d\rho_0 [R^2 + (\rho_0 - \ell_{\text{e,ex}})R] \Delta Z_{\text{ex}}^{(0)}(\rho_0) \quad (29)$$

for a single polymer in the exterior compartment up to and including all terms of order  $R$  with  $\Delta Z_{\text{ex}}^{(0)}$  as in (23).

Performing the final integral over the polymer starting point  $R_0$  leads to

$$\Delta Z_{\text{ex}} = -4\pi R^2 A_2 - 4\pi R A_1 + \mathcal{O}(R^0), \quad (30)$$

with

$$A_2 \equiv \left(\frac{2}{3\pi}\right)^{1/2} R_{\text{p,ex}} + \ell_{\text{e,ex}} \times \operatorname{erfc}\left(\frac{R_{\text{p,ex}}}{6^{1/2}\ell_{\text{e,ex}}}\right) \exp\left(\frac{R_{\text{p,ex}}^2}{6\ell_{\text{e,ex}}^2}\right) - \ell_{\text{e,ex}} \quad (31)$$

and

$$A_1 \equiv \frac{R_{\text{p,ex}}^2}{6} - 2\left(\frac{2}{3\pi}\right)^{1/2} R_{\text{p,ex}}\ell_{\text{e,ex}} - 2\ell_{\text{e,ex}}^2 \times \operatorname{erfc}\left(\frac{R_{\text{p,ex}}}{6^{1/2}\ell_{\text{e,ex}}}\right) \exp\left(\frac{R_{\text{p,ex}}^2}{6\ell_{\text{e,ex}}^2}\right) + 2\ell_{\text{e,ex}}^2. \quad (32)$$

In a similar way, one can calculate the partition function  $Z_{\text{in}}$  of a single polymer of size  $R_{\text{p,in}}$  in the interior vesicle compartment. This partition function is defined via

$$\begin{aligned} Z_{\text{in}} &\equiv 4\pi \int_0^R dR_0 R_0^2 Z_{\text{in}}(R_0) \\ &= 4\pi \int_{-R}^0 d\rho_0 (R + \rho_0) Z_{\text{in}}(R + \rho_0). \end{aligned} \quad (33)$$

We now use the path integral representation for the partition function  $Z_{\text{in}}$ , compare with the corresponding expression (11) for  $Z_{\text{ex}}$ , make the analogous change of variables from  $r_3$  to  $r_3 - l(\underline{r})$ , compare with the transformation from (11) to (13), expand the resulting expression in powers of  $1/R$ , and subtract the constant bulk term. In this way, we arrive at the small curvature expansion for the partition function difference

$$\Delta Z_{\text{in}} = -4\pi R^2 B_2 + 4\pi R B_1 + \mathcal{O}(R^0) \quad (34)$$

with

$$B_2 \equiv \left(\frac{2}{3\pi}\right)^{1/2} R_{\text{p,in}} + \ell_{\text{e,in}} \times \operatorname{erfc}\left(\frac{R_{\text{p,in}}}{6^{1/2}\ell_{\text{e,in}}}\right) \exp\left(\frac{R_{\text{p,in}}^2}{6\ell_{\text{e,in}}^2}\right) - \ell_{\text{e,in}} \quad (35)$$

and

$$B_1 \equiv \frac{R_{\text{p,in}}^2}{6} - 2\left(\frac{2}{3\pi}\right)^{1/2} R_{\text{p,in}}\ell_{\text{e,in}} - 2\ell_{\text{e,in}}^2 \operatorname{erfc}\left(\frac{R_{\text{p,in}}}{6^{1/2}\ell_{\text{e,in}}}\right) \times \exp\left(\frac{R_{\text{p,in}}^2}{6\ell_{\text{e,in}}^2}\right) + 2\ell_{\text{e,in}}^2, \quad (36)$$

which has the same form as (30) apart from the change of sign for the term of order  $R$ .

Note that expressions (30) and (34) for the exterior and the interior compartment both vanish in the limit of small polymer size  $R_{\text{p,ex}}$  and  $R_{\text{p,in}}$ , respectively. Indeed, in the limit of small polymer sizes, there is only a single conformational state of the polymers that is contained in the bulk term and has been subtracted in order to define the partition function differences.

### 4.3. Non-perturbative calculation

For a spherical surface, the partition function of a single polymer can also be calculated in closed form. If one end of the polymer is anchored at distance  $R_0$  from the origin and the spherical vesicle surface has radius  $R$  as before, one obtains the explicit expression [32]

$$\begin{aligned} Z^R(R_0) &= 1 + \frac{1}{(1 + R_0/R)(1 + \ell_e^R/R)} \\ &\times \left[ Z_1^R - \operatorname{erfc}\left(\left(\frac{3}{2}\right)^{1/2} \frac{R_0}{R_p}\right) \right] \end{aligned} \quad (37)$$

with

$$\begin{aligned} Z_1^R &\equiv \operatorname{erfc}\left(\left(\frac{3}{2}\right)^{1/2} \frac{R_0}{R_p} + \frac{1}{6^{1/2}} \left(\frac{R_p}{\ell_e^R} + \frac{R_p}{R}\right)\right) \\ &\times \exp\left(\frac{1}{6} \left(\frac{R_p}{\ell_e^R} + \frac{R_p}{R}\right)^2 + \left(\frac{R_0}{\ell_e^R} + \frac{R_0}{R}\right)\right), \end{aligned} \quad (38)$$

where  $R_p$  and  $\ell_e^R$  are the polymer size and the extrapolation length at the spherical surface, respectively.

The extrapolation length  $\ell_e^R$  depends on the curvature  $1/R$  of the spherical surface. Using a square well

potential and performing the contact potential limit of vanishing potential range and infinite depth, the extrapolation length behaves as  $\ell_e^R \approx \ell_e(1 + \ell_e/R)$  for small curvatures  $1/R$  where  $\ell_e$  is the extrapolation length in the half-space as used above. If one inserts this expansion for the extrapolation length into the partition function as given by (37) and expands the resulting expression in powers of  $1/R$ , one recovers the two expressions (30) and (34) for the exterior and interior vesicle compartment. This provides an explicit check of the perturbative calculation.

## 5. Many polymer chains close to a spherical vesicle

So far, we have considered the partition function of a single polymer chain. We now extend our calculation to the case of many chains. As before, we will consider ideal chains and, thus, ignore the effects of self-avoidance. The basic geometry is again the one sketched in figure 3. The exterior volume accessible to the polymers is given by the spherical shell of thickness  $L$ . Thus, we define the exterior and interior volume by

$$\mathcal{V}_{\text{ex}} \equiv 4\pi((L+R)^3 - R^3)/3 \quad \text{and} \quad \mathcal{V}_{\text{in}} \equiv 4\pi R^3/3, \quad (39)$$

respectively, and the total volume by

$$\mathcal{V} \equiv \mathcal{V}_{\text{ex}} + \mathcal{V}_{\text{in}}. \quad (40)$$

The interior and exterior compartments contain  $N_{\text{ex}}$  and  $N_{\text{in}}$  polymers, respectively.

### 5.1. Osmotic conditions

For dilute solutions and non-interacting polymers, the osmotic pressure difference  $\Delta P$  across the membrane is given by  $\Delta P = T(n_{\text{ex}} - n_{\text{in}})$ , where  $n_{\text{ex}} = N_{\text{ex}}/\mathcal{V}_{\text{ex}}$  is the polymer number density in the exterior compartment, and  $n_{\text{in}} = N_{\text{in}}/\mathcal{V}_{\text{in}}$  is the polymer number density in the interior vesicle compartment. The osmotic pressure can be balanced by choosing the same number density on both sides of the vesicle. The combined grand canonical partition function for the polymers on both sides of the membrane is given by

$$\mathcal{Z}_{\text{G}} = \mathcal{Z}_{\text{G,ex}} \mathcal{Z}_{\text{G,in}}, \quad (41)$$

where  $\mathcal{Z}_{\text{G,ex}}$  and  $\mathcal{Z}_{\text{G,in}}$  are the grand canonical partition functions for the exterior and interior compartment, respectively. For non-interacting polymers as considered, the grand canonical partition functions factorize and can be expressed in terms of the partition

functions  $\mathcal{Z}_i$  with  $i = \text{ex, in}$  for the single polymers. The corresponding expression is given by

$$\mathcal{Z}_{\text{G},i} = \sum_{N_i} \exp(\mu_i N_i/T) \left[ \frac{\mathcal{Z}_i}{\lambda_T^3} \right]^{N_i} \frac{1}{N_i!} = \exp\left( \frac{\zeta_i \mathcal{Z}_i}{\lambda_T^3} \right) \quad (42)$$

with the chemical potentials  $\mu_i$ , the thermal de Broglie wavelength  $\lambda_T \equiv h/(2\pi m_p T)^{1/2}$ , which depends on the Planck constant  $h$  and the polymer mass  $m_p$ , and the fugacities  $\zeta_i \equiv \exp(\mu_i/T)$ , which are connected to the average number of particles in the bulk  $N_{\text{b},i}$  by the relation  $\zeta_i = \lambda_T^3 N_{\text{b},i} / \mathcal{Z}_i$ . Because the bulk term of the single polymer partition function is given by the bulk volume, the fugacities are proportional to the bulk number densities  $n_{\text{b},i}$  of the polymers, and  $\zeta_i = \lambda_T^3 n_{\text{b},i}$ .

Since the osmotic pressures on both sides of the membrane are taken to be equal, we can simplify the notation and put

$$n_{\text{b}} \equiv n_{\text{b,ex}} = n_{\text{b,in}}, \quad \zeta \equiv \zeta_{\text{ex}} = \zeta_{\text{in}} \quad \text{and} \\ \mu \equiv \mu_{\text{ex}} = \mu_{\text{in}}. \quad (43)$$

The grand canonical potential or free energy of the total system is given by

$$\mathcal{F} = -T n_{\text{b}} \mathcal{Z}_{\text{ex}} - T n_{\text{b}} \mathcal{Z}_{\text{in}} \quad (44)$$

and is, thus, expressed in terms of the partition functions  $\mathcal{Z}_{\text{ex}}$  and  $\mathcal{Z}_{\text{in}}$  of a single polymer. Since we are interested in the free energy difference between the system with and without vesicle, we will calculate the grand canonical potential difference  $\Delta \mathcal{F} = \mathcal{F} - \mathcal{F}_{\text{b}}$ , where  $\mathcal{F}_{\text{b}}$  is the grand canonical potential for the bulk system. Our normalization convention implies that the bulk partition function of non-anchored polymers is equal to the volume. This leads to  $\mathcal{F}_{\text{b}} = -T n_{\text{b}} \mathcal{V}$ . The grand canonical free energy difference is thus given by

$$\Delta \mathcal{F} = \mathcal{F} + T n_{\text{b}} \mathcal{V} = -T n_{\text{b}} (\Delta \mathcal{Z}_{\text{ex}} + \Delta \mathcal{Z}_{\text{in}}) \quad (45)$$

with the partition function differences

$$\Delta \mathcal{Z}_{\text{ex}} = \mathcal{Z}_{\text{ex}} - \mathcal{V}_{\text{ex}} \quad \text{and} \quad \Delta \mathcal{Z}_{\text{in}} = \mathcal{Z}_{\text{in}} - \mathcal{V}_{\text{in}} \quad (46)$$

for a single polymer as calculated in section 4.2. In this way, the grand canonical free energy difference for a solution of many chains has been expressed in terms of the partition function differences for a single

chain. An analogous calculation holds for a solution of colloidal particles, for which one has to calculate the partition function for a single colloid, see next section.

## 5.2. Curvature expansion of free energy

The expression (45) for the grand canonical free energy difference is proportional to the membrane area  $A = 4\pi R^2$  and, thus, diverges for large radius  $R$  or small curvature  $1/R$  as  $\sim R^2$ . In order to obtain a regular curvature expansion, it is convenient to consider the corresponding free energy density  $\Delta\mathcal{F}/A$  which is the grand canonical free energy difference per membrane area. A systematic curvature expansion of this quantity is obtained in terms of the two principal curvatures  $1/R_1$  and  $1/R_2$  of the membrane surface which define the mean curvature  $M \equiv (1/2)(1/R_1 + 1/R_2)$  and the Gaussian curvature  $G \equiv 1/R_1 R_2$ . This leads to the general form [8]

$$\Delta\mathcal{F}/A \approx f_0 + f_1 M + f_2 M^2 + f_3 G \quad (47)$$

for small curvatures  $M$  and  $G$ .

For a vesicle in contact with two polymer solutions in the interior and exterior compartment, the first two expansion coefficients  $f_0$  and  $f_1$  can be obtained from the curvature expansions for  $\Delta\mathcal{Z}_{\text{ex}}$  and  $\Delta\mathcal{Z}_{\text{in}}$  as given by (30) and (34). When these latter expressions are inserted into relation (45) for  $\Delta\mathcal{F}$ , one obtains

$$f_0 = Tn_b(A_2 + B_2) \quad (48)$$

with  $A_2$  and  $B_2$  as given by (31) and (35) and

$$f_1 = Tn_b(A_1 - B_1) \quad (49)$$

with  $A_1$  and  $B_1$  as given by (32) and (36).

In order to determine the coefficient  $f_2$  in the curvature expansion (47) of the free energy density, one has to consider the single polymer partition functions both for a spherical and for a cylindrical membrane surface, and expand these partition functions up to order  $R^0$  in the radius  $R$  of the sphere and the cylinder, respectively. This is explicitly done in the next section for aqueous solutions containing non-adhesive nanoparticles or colloids. For solutions containing non-adhesive polymers, the general form  $\Delta\mathcal{F} = -Tn_b(\Delta\mathcal{Z}_{\text{ex}} + \Delta\mathcal{Z}_{\text{in}})$  as given by (45) together with dimensional analysis implies that

$$f_2 = Tn_b R_{\text{p,ex}}^3 \Omega(R_{\text{p,in}}/R_{\text{p,ex}}), \quad (50)$$

where  $R_{\text{p,ex}}$  and  $R_{\text{p,in}}$  denote again the end-to-end distance of the polymers in the exterior and interior compartment, respectively, and  $\Omega(x)$  is a dimensionless function which depends on the ratio  $x = R_{\text{p,in}}/R_{\text{p,ex}}$  of these two length scales.

## 6. Non-adhesive nanoparticles or colloids

In this section, we consider nanoparticles or colloids which are spherical with radius  $R_{\text{c,ex}}$  and  $R_{\text{c,in}}$  in the exterior and interior compartment, respectively. These particles are taken to be non-adhesive and thus experience only hard core interactions with the membrane. In this case, the excess free energies can be easily calculated both for a spherical and for a cylindrical membrane surface.

### 6.1. Spherical membrane surface

First, let us again consider a spherical membrane surface with radius  $R$  as in figure 3 and a single nanoparticle with radius  $R_{\text{c,ex}}$  in the exterior compartment at distance  $R_0$  from the origin with  $R_0 > R + R_{\text{c,ex}}$ . In the limit of large thickness  $L$  of the auxiliary spherical shell, compare figure 3, the partition function for this nanoparticle is simply given by

$$Z_{\text{ex}}^{\text{sp}}(R_0, R) = \theta[R_0 - (R + R_{\text{c,ex}})], \quad (51)$$

where  $\theta(x)$  is the Heaviside step function with  $\theta(x) = 0$  for  $x < 0$  and  $\theta(x) = 1$  for  $x > 0$ . Likewise, the partition function of a single colloid in the interior compartment is equal to

$$Z_{\text{in}}^{\text{sp}}(R_0) = \theta[(R - R_{\text{c,in}}) - R_0]. \quad (52)$$

Inserting these expressions into (27) and (33) leads to the single colloid partition functions, which correspond to the volumes accessible to these particles. Therefore, one obtains  $Z_{\text{ex}}^{\text{sp}} = 4\pi(L + R)^3/3 - 4\pi(R + R_{\text{c,ex}})^3/3$  and  $Z_{\text{in}}^{\text{sp}} = 4\pi(R - R_{\text{c,in}})^3/3$  for the exterior and interior compartment, respectively.

If we subtract the bulk terms which are equal to the exterior and interior volume, respectively, we obtain the partition function differences

$$\Delta Z_{\text{ex}}^{\text{sp}} = -4\pi R_{\text{c,ex}} R^2 - 4\pi R_{\text{c,ex}}^2 R - \frac{4\pi}{3} R_{\text{c,ex}}^3 \quad (53)$$

and

$$\Delta Z_{\text{in}}^{\text{sp}} = -4\pi R_{\text{c,in}} R^2 + 4\pi R_{\text{c,in}}^2 R - \frac{4\pi}{3} R_{\text{c,in}}^3. \quad (54)$$

The grand canonical free energy difference per unit area is now given by

$$\Delta\mathcal{F}^{\text{sp}} = -Tn_b\Delta\mathcal{Z}_{\text{ex}}^{\text{sp}} - Tn_b\Delta\mathcal{Z}_{\text{in}}^{\text{sp}} \quad (55)$$

as follows from (45).

The spherical surface has constant mean curvature  $M = 1/R$  and constant Gaussian curvature  $G = 1/R^2$ , and the curvature expansion (47) of the free energy difference now has the form

$$\Delta\mathcal{F}^{\text{sp}}/\mathcal{A} \approx f_0 + f_1/R + (f_2 + f_3)/R^2. \quad (56)$$

Using the explicit expressions (53) and (54) for  $\Delta\mathcal{Z}_{\text{ex}}^{\text{sp}}$  and  $\Delta\mathcal{Z}_{\text{in}}^{\text{sp}}$ , we thus arrive at the expansion coefficients

$$f_0 = Tn_b(R_{\text{c,ex}} + R_{\text{c,in}}), \quad (57)$$

$$f_1 = Tn_b(R_{\text{c,ex}}^2 - R_{\text{c,in}}^2) \quad (58)$$

and the relation

$$f_2 + f_3 = \frac{1}{3}Tn_b(R_{\text{c,ex}}^3 + R_{\text{c,in}}^3). \quad (59)$$

### 6.2. Cylindrical membrane surface

In order to determine the values of  $f_2$  and  $f_3$ , we need another relation for these two coefficients which can be obtained by repeating the same calculation for a cylindrical membrane surface. The radius of this cylinder is again denoted by  $R$ , the corresponding membrane area by  $\mathcal{A}$ . As a result, one obtains

$$\Delta\mathcal{Z}_{\text{ex}}^{\text{cy}}/\mathcal{A} = -R_{\text{c,ex}} - R_{\text{c,ex}}^2/2R, \quad (60)$$

$$\Delta\mathcal{Z}_{\text{in}}^{\text{cy}}/\mathcal{A} = -R_{\text{c,in}} + R_{\text{c,in}}^2/2R \quad (61)$$

and

$$\Delta\mathcal{F}^{\text{cy}}/\mathcal{A} = Tn_b(R_{\text{c,ex}} + R_{\text{c,in}}) + Tn_b(R_{\text{c,ex}}^2 - R_{\text{c,in}}^2)/2R. \quad (62)$$

The cylindrical surface has constant mean curvature  $M = 1/2R$  and zero Gaussian curvature  $G = 0$ , and the curvature expansion (47) of the free energy difference has the form

$$\Delta\mathcal{F}^{\text{cy}}/\mathcal{A} \approx f_0 + f_1/2R + f_2/2R^2. \quad (63)$$

Comparing this expansion with the explicit expression (62), we recover the two expansion coefficients  $f_0$  and  $f_1$  as obtained for the spherical surface. In addition, the coefficient  $f_2$  of the  $M^2$ -term in the curvature expansion of the free energy is simply given by

$$f_2 = 0. \quad (64)$$

It then follows from (59) that

$$f_3 = \frac{1}{3}Tn_b(R_{\text{c,ex}}^3 + R_{\text{c,in}}^3). \quad (65)$$

The vanishing of  $f_2$  is related to the fact that the curvature expansion of the excluded volume in front of a curved surface contains no term proportional to  $M^2$  as previously noticed in [20].

### 7. Particle-induced membrane curvature

We now study the interplay between the entropy of the polymers or nanoparticles and the bending energy of the membrane. As before, the membrane is described as a two-dimensional surface which divides space into an interior and exterior compartment. For a symmetric membrane, the bending energy of the membrane surface depends on the bending rigidity  $\kappa$  and the Gaussian modulus  $\kappa_G$  and is given by [33]

$$\mathcal{E}_{\text{me}} = \oint d\mathcal{A}(2\kappa M^2 + \kappa_G G), \quad (66)$$

where the area integral extends over the whole membrane area and the mean curvature  $M$  and the Gaussian curvature  $G$  will, in general, depend on the local surface coordinates.

For a spherical and a cylindrical shape, one has constant curvatures which implies the bending energy per membrane area

$$\mathcal{E}_{\text{me}}/\mathcal{A} = 2\kappa M^2 + \kappa_G G. \quad (67)$$

The total free energy density of the spherical or cylindrical membrane surface in contact with the particle dispersion is then given by

$$(\Delta\mathcal{F} + \mathcal{E}_{\text{me}})/\mathcal{A} \approx f_0 + f_1 M + (2\kappa + f_2)M^2 + (\kappa_G + f_3)G \quad (68)$$

for small curvatures  $M$  and  $G$ . Minimization of this free energy density with respect to  $M$  for fixed  $G$  [8] leads to the particle-induced curvature

$$M_{\text{ind}} = -f_1/(4\kappa + 2f_2) \equiv M_{\text{sp}}, \quad (69)$$

which we identify with the ‘spontaneous’ curvature  $M_{\text{sp}}$  of the membrane.

For a dispersion of non-adhesive nanoparticles or colloids as considered in the previous section, one has  $f_2 = 0$  and  $M_{\text{sp}} = -f_1/4\kappa$ . In general, the expansion coefficient  $f_2$  will be non-zero and will then lead to the effective bending rigidity

$$\kappa_{\text{eff}} \equiv \kappa + f_2/2 \quad (70)$$

and the spontaneous curvature

$$M_{\text{sp}} = -f_1/4\kappa_{\text{eff}}. \quad (71)$$

If both the exterior and the interior vesicle compartments contain non-adhesive particles that have essentially the same linear size,  $R_{\text{pa}}$ , it follows from relations (50) and (59) that  $f_2 \sim Tn_b R_{\text{pa}}^3 \sim T\phi$  where  $\phi$  is the volume fraction of the particle dispersion. For dilute solutions as considered here, the volume fraction  $\phi \ll 1$  and

$$f_2 \ll T. \quad (72)$$

Furthermore, for lipid bilayers, the bending rigidity  $\kappa$  is large compared to  $T$  and the effective bending rigidity  $\kappa_{\text{eff}}$  is rather close to  $\kappa$ .

### 7.1. Two species of polymers

First, consider two polymer solutions in the exterior and interior compartment with different polymer radii  $R_{\text{p,ex}}$  and  $R_{\text{p,in}}$ , respectively, and assume that the exterior polymers are adsorbing onto the membrane whereas the interior polymers are non-adsorbing, see figure 1. In this case, expression (71) for the polymer-induced curvature leads to

$$M_{\text{sp}} = -\frac{T}{4\kappa_{\text{eff}}} n_b \left[ \frac{1}{6} (R_{\text{p,ex}}^2 - R_{\text{p,in}}^2) - \left( \frac{8}{3\pi} \right)^{1/2} R_{\text{p,ex}} \ell_{\text{e,ex}} - 2\ell_{\text{e,ex}}^2 [\text{erfc}(\bar{R}) \exp(\bar{R}^2) - 1] \right] \quad (73)$$

with the reduced polymer size

$$\bar{R} \equiv R_{\text{p,ex}}/6^{1/2}\ell_{\text{e,ex}}. \quad (74)$$

In figure 4, the membrane curvature is plotted as a function of the adsorption strength between polymers and membranes for vanishing  $R_{\text{p,in}}$  (the radius of polymers inside the vesicle). In this case, the curvature effect arises from the adsorption–desorption behaviour of the exterior polymers. In the strong desorption limit, the spontaneous curvature attains  $M_{\text{sp}} = -TR_{\text{p,ex}}^2 n_b / 24\kappa_{\text{eff}}$ . Thus, our theory predicts that the membrane bends *towards* the polymers in agreement with the results obtained in [19] and in [20] but in disagreement with those in [27].

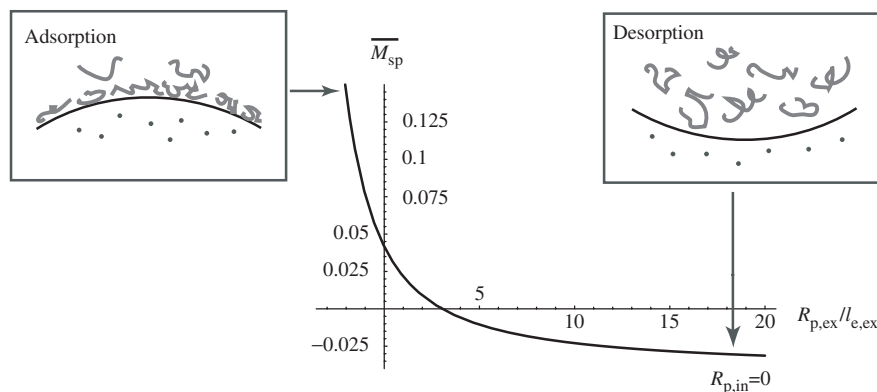


Figure 4. Polymer-induced membrane curvature  $M_{\text{sp}}$  as a function of the inverse extrapolation length  $1/\ell_{\text{e,ex}}$  for a vesicle in contact with an exterior solution of adsorbing polymers and an interior solution of desorbing polymers (or colloids). The functional dependence shown in this figure corresponds to the limit of small size of the interior polymers (or colloids). The spontaneous curvature is rescaled according to  $\bar{M}_{\text{sp}} \equiv \kappa_{\text{eff}} M_{\text{sp}} / T n_b R_{\text{p,ex}}^2$  with the temperature  $T$  in energy units, the bulk particle number density  $n_b$ , which is identical in both compartments, and the end-to-end distance  $R_{\text{p,ex}}$  of the exterior polymers. If the polymers are adsorbed to the membrane surface (left) and desorbed from this surface (right), the membrane bends away from and towards the polymers, respectively. The polymer-induced curvature changes its sign at  $R_{\text{e,ex}}/\ell_{\text{e,ex}} \simeq 3.04$ .

The behaviour of non-anchored polymers differs from the situation of anchored polymers, in which the membrane bends *away* from the polymers in the non-adsorbing case [7]. This difference reflects the fact that non-anchored polymers influence the membrane both by their configurational and by their translational degrees of freedom and thus, by the depletion volume close to the membrane. As a consequence, if the membrane bends towards the solution the volume of the depletion zone is decreased compared to the flat situation, see the schematic picture in the inset on the right side of figure 4.

In the limit of strong adsorption, i.e. for large negative  $1/\ell_{e,ex}$ , the membrane bends *away* from the polymer solution in order to increase the volume of the adsorption layer above the membrane surface, see the left inset of figure 4. The curvature in this direction does not saturate, since the volume can be increased further for stronger bending. The same sign of the particle-induced curvature is found for adhesive nanoparticles [20].

If one starts in the regime of adsorbed polymers and decreases the strength of the attractive potential between polymers and membrane, the curvature is a monotonic function of the potential strength. For  $R_{p,ex}/\ell_{e,ex} = 0$ , i.e. at the adsorption/desorption transition of polymers in the vicinity of a flat surface, the membrane curvature is given by  $M_{sp} = TR_{p,ex}^2 n_b / 24\kappa_{eff}$  and thus has the same amplitude as the induced curvature in the strong

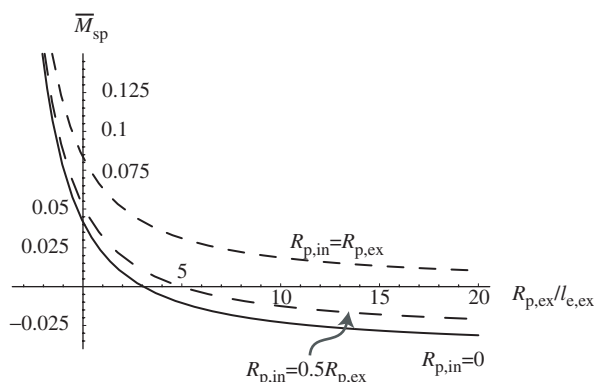


Figure 5. Particle-induced membrane curvature  $M_{sp}$  as a function of the inverse extrapolation length  $1/\ell_{e,ex}$  for a vesicle in contact with an exterior solution of adsorbing polymers and an interior solution of desorbing polymers (or colloids). The rescaling of the spontaneous curvature is the same as in figure 4. The three curves correspond to three different sizes  $R_{p,in}$  of the interior polymers. As one increases the ratio  $R_{p,in}/R_{p,ex}$  of the interior polymer size to the exterior one, the point at which the membrane curvature changes its sign is shifted towards larger values of  $R_{p,ex}/\ell_{e,ex}$ . For  $R_{p,in} = R_{p,ex}$ , the membrane curvature vanishes for large positive  $R_{p,ex}/\ell_{e,ex}$ , i.e. in the limit of total desorption.

desorption limit but with opposite sign. Thus, for  $R_{p,ex}/\ell_{e,ex} = 0$ , the membrane is still bent away from the polymers. This is understandable since the positive membrane curvature leads to additional configurational space for the polymers and therefore leads to an increase of the monomer density in the vicinity of the membrane surface, corresponding to stronger adsorption. The membrane curvature changes its sign for  $R_{p,ex}/\ell_{e,ex} \approx 3.04$ : in order to avoid any curvature effect arising from the polymer solution, one has to go beyond the adsorption–desorption transition and enter the desorption regime.

In figure 5, the membrane curvature is plotted as a function of the inverse extrapolation length for different values of the interior polymer size. The spontaneous curvature increases with increasing size of the interior polymers. If the polymers in the interior and exterior compartment have the same size and both polymer species are totally desorbed, the polymer-induced curvature vanishes as expected.

## 7.2. Adsorbed polymers and desorbed colloids

If the exterior volume contains adsorbing polymers of radius  $R_{p,ex}$  and the interior volume contains desorbed colloids or nanoparticles of radius  $R_{c,in}$ , expression (71) leads to the particle-induced curvature

$$M_{sp} = -\frac{T}{4\kappa_{eff}} n_b \left[ \frac{1}{6} R_{p,ex}^2 - R_{c,in}^2 - \left( \frac{8}{3\pi} \right)^{1/2} R_{p,ex} \ell_{e,ex} - 2\ell_{e,ex}^2 [\operatorname{erfc}(\bar{R}) \exp(\bar{R}^2) - 1] \right] \quad (75)$$

with  $\bar{R} = R_{p,ex}/6^{1/2}\ell_{e,ex}$  as before. Comparison with equation (73) shows that desorbed colloids have the same effect on the membrane curvature as desorbed polymers if the colloid size and the polymer size satisfy the relation  $R_{c,in}^2 = R_{p,in}^2/6$ .

It follows from relations (73) and (75) that an increase in the colloid size  $R_{c,in}$  and in the polymer size  $R_{p,in}$  within the interior compartment leads to an increase in the membrane curvature. In the limit of total desorption, i.e. when the inverse extrapolation length  $1/\ell_{e,ex} \gg 1$ , one obtains

$$M_{sp} = -\frac{T}{4\kappa_{eff}} n_b R_{p,ex}^2 \left[ \frac{1}{6} - \left( \frac{R_{c,in}}{R_{p,ex}} \right)^2 \right] = -\frac{T}{24\kappa} n_b R_{p,ex}^2 \left[ 1 - \left( \frac{R_{p,in}}{R_{p,ex}} \right)^2 \right] \quad (76)$$

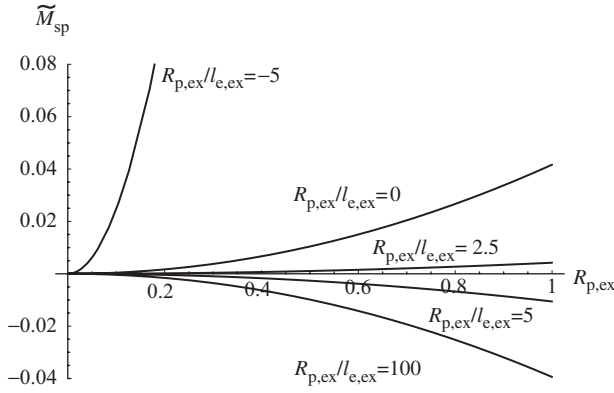


Figure 6. The polymer-induced curvature  $\tilde{M}_{sp} \equiv \kappa_{\text{eff}} M_{sp} / T n_b$  as a function of the polymer size  $R_{p,\text{ex}}$  in the exterior compartment in the limit in which the size of the interior particles is small. The different curves correspond to different values of the extrapolation length  $\ell_{e,\text{ex}}$ .

for colloids and polymers in the interior compartment, respectively. This curvature vanishes for  $R_{c,\text{in}} = R_{p,\text{ex}} / \sqrt{6}$ , and for  $R_{p,\text{in}} = R_{p,\text{ex}}$ .

In figure 6, the dependence of the polymer-induced curvature on the polymer radius of the exterior polymers is shown for vanishing particle radii in the interior compartment. As expected, for all values of the inverse extrapolation length, the curvature effect vanishes in the limit of small  $R_{p,\text{ex}}$ .

### 7.3. Two species of desorbed colloids

If one has two species of desorbed colloids or nanoparticles with different radii  $R_{c,\text{ex}}$  and  $R_{c,\text{in}}$  in the exterior and interior compartment, expression (71) leads to the particle-induced curvature

$$M_{sp} = -\frac{T}{4\kappa} n_b [R_{c,\text{ex}}^2 - R_{c,\text{in}}^2], \quad (77)$$

where we have used the fact that  $\kappa_{\text{eff}} = \kappa$  since the expansion coefficient  $f_2 = 0$  in this case. As one can easily deduce from this equation, the membrane bends towards the larger colloids as previously shown in [20]. In the latter reference, the finite membrane thickness  $\ell_{\text{me}}$  was taken into account which leads to

$$M_{sp} = -\frac{T}{4\kappa} n_b (R_{c,\text{ex}} - R_{c,\text{in}}) (\ell_{\text{me}} + R_{c,\text{ex}} + R_{c,\text{in}}). \quad (78)$$

If both colloidal species have the same size, the curvature of the membrane vanishes as expected.

## 8. Conclusion and outlook

We have shown that the curvature of membranes is strongly influenced by polymers and colloids which are dispersed in the surrounding solution. We focused on the experimentally relevant situation of vesicles which are osmotically balanced and considered particles of different sizes and adsorption behaviour on both sides of the vesicle membrane. The particle-induced membrane curvature was calculated as a function of the adsorption strength.

For two different particle species, which are totally desorbed from the membrane surface, the membrane bends towards the larger particles. If the particles in the exterior compartment are adhesive, the curvature is increased, such that the membrane bends away from the strongly adsorbed particles. This is due to the translational entropy of the non-anchored particles. For strong desorption, the depletion volume above the membrane is reduced (relative to the membrane area), if the membrane bends towards the desorbed particles. For strong adsorption, the membrane bends away from the adsorbed polymers in order to increase the area of the adsorption layer. All of these results agree with those obtained previously in [20] by different arguments based on the interfacial tensions of the two membrane–water interfaces.

The results obtained here for the polymer-induced curvature are valid in the whole range between the strong adsorption and the complete desorption regime. The adsorption strength is described in terms of the inverse extrapolation length  $1/\ell_e$ . As one varies this parameter from large negative values, corresponding to strong adsorption, to large positive values, corresponding to complete desorption, one encounters a certain characteristic value at which the polymer-induced curvature vanishes, see figures 4 and 5. This provides the possibility to switch the polymer-induced curvature from positive to negative values by reducing the adsorption strength.

Inspection of figures 4 and 5 shows that the polymer-induced curvature vanishes at a positive value of the inverse extrapolation length  $1/\ell_e$ , which corresponds to a desorbed state at the flat membrane. For  $1/\ell_e = 0$ , on the other hand, which corresponds to the adsorption–desorption transition point of the flat membrane, the polymer-induced curvature is positive and the membrane bends away from the adsorbed polymers. The vanishing of the polymer-induced curvature at positive values of  $1/\ell_e$  reflects the interplay between translational and configurational entropy of the polymers.

Another situation studied here is a vesicle which is in contact with nanoparticles of radius  $R_{c,\text{in}}$  in the interior

compartment and with polymers characterized by their end-to-end distance  $R_{p,ex}$  in the exterior compartment. In the complete desorption limit, the effects of the nanoparticles and the polymers cancel for  $R_{c,in} = R_{p,ex}/6^{1/2}$ . All of these curvature effects should be accessible to experiments if one studies the shape and the shape fluctuations of the vesicle as has been demonstrated for vesicles in contact with two different sugar solutions [34].

RL takes this opportunity to thank Ben Widom for much advice and helpful correspondence over many years.

### Appendix A: Glossary: list of symbols

|                    |   |
|--------------------|---|
| $\mathcal{A}$      | membrane area   |
| $\mathcal{E}_{me}$ | bending energy of membrane configuration                        |
| $f_n$              | expansion coefficients of free energy                           |
| $\mathcal{F}$      | grand canonical potential or free energy                        |
| $G$                | Gaussian curvature  |
| $\kappa$           | bending rigidity  |
| $\kappa_G$         | Gaussian modulus  |
| $L$                | thickness of auxiliary spherical shell around spherical vesicle |
| $\ell_e$           | extrapolation length  |
| $\lambda_T$        | thermal de Broglie wavelength                                   |
| $M$                | mean curvature  |
| $M_{sp}$           | spontaneous curvature   |
| $\mu$              | chemical potential  |
| $n$                | number density of particles                                     |
| $n_b$              | bulk number density of particles                                |
| $\mathbf{n}$       | normal vector   |
| $N_{in}$           | number of particles in the interior compartment                 |
| $N_{ex}$           | number of particles in the exterior compartment                 |
| $N$                | monomer number of polymer                                       |
| $P$                | osmotic pressure  |
| $\mathbf{r}(s)$    | three-dimensional spatial position of monomer $s$               |
| $\underline{r}(s)$ | lateral position of monomer $s$                                 |
| $r_3(s)$           | perpendicular position of monomer $s$                           |
| $R$                | curvature radius of vesicle                                     |
| $R_0$              | distance of polymer anchor point from origin                    |
| $R_c$              | radius of spherical nanoparticle or colloid                     |
| $R_p$              | end-to-end distance of polymer                                  |
| $s$                | internal (contour) length of polymer                            |
| $T$                | absolute temperature (in energy units)                          |
| $V$                | interaction potential between polymer and membrane              |
| $\mathcal{V}$      | total volume  |
| $\mathcal{V}_{in}$ | volume of interior compartment                                  |
| $\mathcal{V}_{ex}$ | volume of exterior compartment                                  |
| $\underline{x}$    | lateral coordinates $x_1, x_2$                                  |
| $z$                | perpendicular coordinate  |
| $Z_G$              | grand canonical partition function                              |

|               |   |
|---------------|---|
| $Z$           | partition function of anchored polymer      |
| $Z_{hs}$      | half-space polymer partition function       |
| $Z''$         | coefficients of curvature expansion of $Z$  |
| $\mathcal{Z}$ | partition function of non-anchored particle |
| $\zeta$       | fugacity                                    |

### References

- [1] R. Lipowsky. *Colloids Surf. A*, **128**, 255 (1997).
- [2] H.-G. Döbereiner, A. Lehmann, W. Goedel, O. Selchow, R. Lipowsky. *Mat. Res. Soc. Symp. Proc.*, **489**, 101 (1998).
- [3] V. Frette, I. Tsafirir, M.-A. Guedeau-Boudeville, L. Jullien, D. Kandel, J. Stavans. *Phys. Rev. Lett.*, **83**, 2465 (1999).
- [4] C. Ligoure, G. Bouglet, G. Porte. *Phys. Rev. Lett.*, **71**, 3600 (1993).
- [5] Y.-M. Tricot, J.H. Fendler. *J. phys. Chem.*, **90**, 3369 (1983).
- [6] F.C. Meldrum, B.R. Heywood, S. Mann. *J. colloid Interface Sci.*, **161**, 66 (1993).
- [7] R. Lipowsky. *Europhys. Lett.*, **30**, 197 (1995).
- [8] C. Hiergeist, R. Lipowsky. *J. Phys. II*, **6**, 1465 (1996).
- [9] R. Lipowsky, H.-G. Döbereiner, C. Hiergeist, V. Indrani. *Physica A*, **249**, 536 (1998).
- [10] M. Breidenich, R.R. Netz, R. Lipowsky. *Europhys. Lett.*, **49**, 431 (2000).
- [11] T. Bickel, C. Marques, C. Jeppsen. *Phys. Rev. E*, **62**, 1124 (2000).
- [12] T. Auth, G. Gompper. *Phys. Rev. E*, **68**, 051801 (2003).
- [13] G. Gompper, H. Edo, M. Mihailescu, J. Allgaier, M. Monkenbusch, D. Richter, B. Jakobs, T. Sottmann, R. Strey. *Europhys. Lett.*, **56**, 683 (2001).
- [14] R. Lipowsky. *J. biol. Phys.*, **28**, 195 (2002).
- [15] C. Hiergeist, V.A. Indrani, R. Lipowsky. *Europhys. Lett.*, **36**, 491 (1996).
- [16] M. Breidenich, R.R. Netz, R. Lipowsky. *Eur. Phys. J. E*, **5**, 403 (2001).
- [17] Y.M. Kim, W. Sung. *Phys. Rev. E*, **63**, 041910 (2001).
- [18] S. Asakura, F. Oosawa. *J. Polym. Sci.*, **33**, 183 (1958).
- [19] E. Eisenriegler, A. Hanke, S. Dietrich. *Phys. Rev. E*, **54**, 1134 (1996).
- [20] R. Lipowsky, H.-G. Döbereiner. *Europhys. Lett.*, **43**, 219 (1998).
- [21] P.G. de Gennes. *J. phys. Chem.*, **94**, 8407 (1990).
- [22] J.T. Brooks, C.M. Marques, M.E. Cates. *Europhys. Lett.*, **14**, 713 (1991).
- [23] J.T. Brooks, C.M. Marques, M.E. Cates. *J. Phys. II*, **1**, 673 (1991).
- [24] F. Clement, J.-F. Joanny. *J. Phys. II*, **7**, 973 (1997).
- [25] T. Garel, M. Kardar, H. Örländ. *Europhys. Lett.*, **29**, 303 (1995).
- [26] M. Laradji. *Europhys. Lett.*, **47**, 694 (1999).
- [27] R. Podgornik. *Europhys. Lett.*, **21**, 245 (1993).
- [28] K. Yaman, P. Pincus, F. Solis, T.A. Witten. *Macromolecules*, **30**, 1173 (1997).
- [29] P.G. de Gennes. *Rep. Prog. phys.*, **32**, 187 (1969).
- [30] E. Eisenriegler. *Polymers Near Surfaces*, World Scientific, Singapore (1993).
- [31] Y. Lepine, A. Caille. *Can. J. Phys.*, **56**, 403 (1978).
- [32] V.A. Indrani, R. Lipowsky. unpublished.
- [33] W. Helfrich. *Z. Naturforsch.*, **28c**, 693 (1973).
- [34] H.G. Döbereiner, O. Selchow, R. Lipowsky. *Eur. Biophys. J.*, **28**, 174 (1999).